

Enhancing Few-Shot Image Classification with Cosine Transformer

Quang-Huy Nguyen¹, Cuong Q. Nguyen¹, Dung D. Le²,
Hieu H. Pham^{1,2,*}, and Minh N. Do^{1,3}

¹ VinUni-Illinois Smart Health Center, VinUniversity, Hanoi, Vietnam;
{huy.nq,cuong.nq,hieu.ph,dung.ld}@vinuni.edu.vn

² College of Engineering & Computer Science, VinUniversity, Hanoi, Vietnam;

³ University of Illinois at Urbana-Champaign, US;

minhdo@illinois.edu

*Corresponding author

Abstract. This paper addresses the few-shot image classification problem. One notable limitation of few-shot learning is the variation in describing the same category, which might result in a significant difference between small labeled support and large unlabeled query sets. Our approach is to obtain a relation heatmap between the two sets in order to label the latter one in a transductive setting manner. This can be solved by using cross-attention with the scaled dot-product mechanism. However, the magnitude differences between two separate sets of embedding vectors may cause a significant impact on the output attention map and affect model performance. We tackle this problem by improving the attention mechanism with cosine similarity. Specifically, we develop FS-CT (Few-shot Cosine Transformer), a few-shot image classification method based on prototypical embedding and transformer-based framework. The proposed Cosine attention improves FS-CT performances significantly from nearly 5% to over 20% in accuracy compared to the baseline scaled dot-product attention in various scenarios on three few-shot datasets *mini*-ImageNet, CUB-200, and CIFAR-FS. Additionally, we enhance the prototypical embedding for categorical representation with learnable weights before feeding them to the attention module. Our proposed method FS-CT along with the Cosine attention is simple to implement and can be applied for a wide range of applications. Our codes are available at <https://github.com/vinuni-vishc/Few-Shot-Cosine-Transformer>.

1 Introduction

In this paper, we seek to tackle the few-shot image classification problem, which aims to recognize unseen categories with minimal labeled samples [10, 18, 32, 33]. Few-shot learning methods can be essential in a wide range of research,

especially in medical image segmentation [17, 35], anomaly detection [23, 31], or security supervision [42, 43], where data is limited due to expensiveness, scarcity, or privacy/security concerns. A standard few-shot learning problem [27, 34, 38, 45], generally, includes two major sets: a labeled *support set* that provides just small sample images describing the category and the unlabeled *query set* to perform the task, in this case, categorical classification. Both sets are then split into two groups, disjoint in categories, for training and evaluating the few-shot method.

Challenge. Previous studies on few-shot classification [11, 19, 26, 40] can be split into two main approaches: (i) learning a distance function over data points on a learnable embedding space [26, 38, 40], and (ii) fine-tuning learned parameters effectively for novel tasks [11, 19, 27]. Since the supporting data is limited, a good embedding is often required to tackle the few-shot problem effectively. However, while few-shot learning may be an effective solution for the limited data problems, there are two critical challenges that we address in this paper: (i) a few samples of support are unable to fully describe the category under different visual variations (e.g., appearance, viewpoint, or shape) and (ii) support and query samples may significantly differ under different variations as in the first challenge. This may constrain current few-shot learning methods’ learning ability significantly under various few-shot tasks.

Approach. To develop an effective method for few-shot learning problems, a pivotal step is obtaining a well-represented relational matrix between the labeled set and unlabeled set to perform tasks on the latter one. One effective approach is utilizing the attention mechanism [8, 20], the core of transformer architectures, for the relational map. There are two main variants for the mechanism: cross-attention calculates the external association between two sets of features, and self-attention calculates the internal relationship within one set. In this work, our core idea to tackle the few-shot image classification task is utilizing the cross-attention mechanism between support and query sets to classify the queries. To obtain good representatives for the support set, the prototypical embedding [32] is applied, as it comes with a well-represented feature for individual classes with low computation cost. The prototypical embedding along with the cross-attention mechanism are two main components of our proposed framework in this study.

However, the two mentioned few-shot challenges above limit these framework components significantly. As the small number of support samples cannot represent the full extent of the category, the arithmetic mean approach is unreliable for prototypical embedding when the support samples, chosen randomly, might be in the margin of the data distribution with unpopular selected samples. This may make the prototypical representations unrepresented. On the other hand, the differences between support and query features might lead to differences in features

and thus affect the performance of the cross-attention map a great deal when using the standard attention mechanism scaled dot-product [37]. We notice that these limitations haven't been tackled in previous studies. Therefore, we made two improvements based on these limitations: (i) propose a weight averaging method with learnable weight replacing the arithmetic mean of the prototypical embedding, and (ii) eliminate the differences in magnitude between two feature sets with a proposed cosine attention mechanism. These two improvements are incorporated in our proposed Few-shot Cosine Transformer (FS-CT).

To evaluate the effectiveness of our proposed method, we developed a detailed empirical evaluation scheme on various settings, configurations, and backbone networks. Our FS-CT with two attention mechanisms: the baseline scaled-dot product attention (which is called "Softmax attention" in this study) and the improved "Cosine attention" are evaluated on three few-shot datasets *mini-ImageNet*, CUB-200, and CIFAR-FS under various backbones and different settings. We further utilized another attention-based few-shot image classification CrossTransformer (CTX) [8] as the baseline method for comparison under the same evaluation scheme, also validating our proposed cosine attention on the other method. Based on the detailed evaluation scheme, we conducted an ablation study on the impact of our improvement in the method's performance. Furthermore, we developed a few-shot dataset describing yoga poses with 50 categories with arbitrary image size and variations, which somewhat reflect the actual data, as a customized dataset to evaluate methods' performance and served as an initial step of conducting research for health-related yoga monitoring problems.

Contributions. In summary, our contributions in this paper include:

- We propose a few-shot image classification method called FS-CT, which consists of the learnable prototypical embedding and Cosine Transformer, with Cosine attention as the heart of the latter module. Rather than designing a new transformer-based architecture, we focus on improving the attention mechanism for better learning capability. Our FS-CT outperforms the baseline CTX [8] in various experiments and achieves a considerable performance on *mini-ImageNet*, CUB-200, and CIFAR-FS datasets.
- We improve the *prototypical embedding* by making it learnable with weight averaging operation. This helps improve categorical representations for the support set and alleviates the impact of variations in support samples for the few-shot task.
- We develop a new attention mechanism called *Cosine attention* to enhance the cross-attention mechanism. By using cosine similarity, we remove the effect of the difference in magnitude between two different input sets of features. This helps output a more stable attention map and improves the transformer performance significantly.

- We also develop a custom few-shot dataset for yoga poses, which not only provides an application experiment for our method but also prepares our future research on healthcare monitoring for Yoga. We make the dataset publicly available at <https://github.com/vinuni-vishc/Few-Shot-Cosine-Transformer>.

Organization. In the following, Section 2 reviews previous studies; Section 3 provides a mathematical formulation of the few-shot classification problem and specifies the proposed FS-CT with cosine attention mechanism; Section 4 presents our experimental settings and evaluation; Section 5 discusses limitations and future works; and Section 6 concludes our contributions paper.

2 Related Work

This section summarizes previous approaches of few-shot learning and attention mechanism, along with their perspective limitations.

Few-shot Learning Few-shot learning is a subset of meta-learning [12, 27, 33], which develops models that are able to adapt to unseen tasks with small training data. Meta-learning algorithms take an advance on prior knowledge from a large-scale dataset (*e.g.*, a pre-trained deep network) to effectively learn on a small novel dataset via a *meta-learner* (or *few-shot learner*) [10, 11, 27, 33]. Based on the learning method, few-shot learning algorithms can be divided into two categories: (1) *Metric-based learning* [5, 16, 26, 32, 34, 38, 40] learns an embedding space that samples from the same category are mapped to points that close together and vice versa under a distance metric. (2) *Optimization-based learning* [11, 12, 19, 27, 33, 45] fine-tune model’s parameters to quickly adapt to the new task with only a few effective gradient descent steps. Metric-based learning is the most simple yet effective method among the two, which usually consists of two stages: *feature extraction* to obtain extracted features from both labeled and unlabeled samples under the same embedding space, and *metric function* to utilize a similarity or distance metric for categorizing unlabeled samples by comparing [34] or clustering [32] the embedded features.

Based on the test settings, there are two learning approaches for few-shot algorithm, including *inductive learning* [11, 30, 34, 38] and *transductive learning* [1, 8, 16, 21, 25]. Inductive learning classifies each query sample individually, while transductive learning classifies every query sample collectively [3]. The latter learning method allows additional information in data distribution or visual resemblance can be obtained and leveraged among query samples, thus potentially improving the overall performance.

In this study, we consider the metric-based learning for our proposed few-shot learner (classifier) Few-shot Cosine Transformer, when our core idea is utilizing

the relationship between support and query features under an embedding space for making predictions. As the performance of few-shot learning task can improve when the meta-learner is built on top of an effective embedding extractor [7, 36], we consider using a pre-trained model for the feature extraction of our FS-CT. Due to the characteristic of the attention mechanism of exploiting the similarity matrix between all support and query samples at once, we consider the transductive learning approach for our method.

Cross-attention mechanism After being introduced in [37] for natural language processing tasks, transformer soon rose to dominance in computer vision [4, 6, 9]. The core of transformer is the attention mechanism, which calculates an attention map that indicates the similarity between features for solving tasks. The mechanism comes with two variants, *self-attention* determines the internal relationships within a feature set, and *cross-transformer* calculates the external relationships between two feature sets. Several few-shot learning studies are inspired by transformer and its attention mechanism [8, 14, 20, 41, 44], where the methods, in general, involve attention mechanism to align labeled and unlabeled feature for classification. While attention is a powerful mechanism, it has critical problems of missing good insight about attention and an expensive quadratic computational cost. Thus, research on the attention mechanism focus on three main directions: (i) reducing the computation cost, (ii) obtaining a good insight for attention, and (iii) designing a good attention mechanism for a specific task. Most studies on attention often focus on the self-attention mechanism with one set of features as input rather than two in cross-attention. Therefore, the difference between two feature sets that might happen in cross-attention becomes unnoticed. This made the attention output becomes unstable, thus reducing the transformer performance.

In this study, we explore deeply this phenomenon inside the scaled dot-product attention mechanism and propose a novel mechanism called cosine attention to tackle the problem. Although prior research has utilized the cross-attention mechanism for few-shot learning, in this work, we are the first to investigate deeply the cross-attention limitation for the few-shot classification problem. To the best of our knowledge, this is the first time the cosine attention mechanism has been explored and prove its effectiveness in the tasks of few-shot learning.

3 Proposed Method

3.1 Problem formulation and notations

We first formalize a standard few-shot classification problem while introducing some notations. Given a train set D_{train} and few-shot learner $A(\cdot | \theta)$. The

objective of few-shot classification is to learn the optimal parameter θ^* so that it can achieve a good performance of algorithm $A(\cdot | \theta)$ on a test set D_{test} . D_{train} and D_{test} must be disjointed in categories.

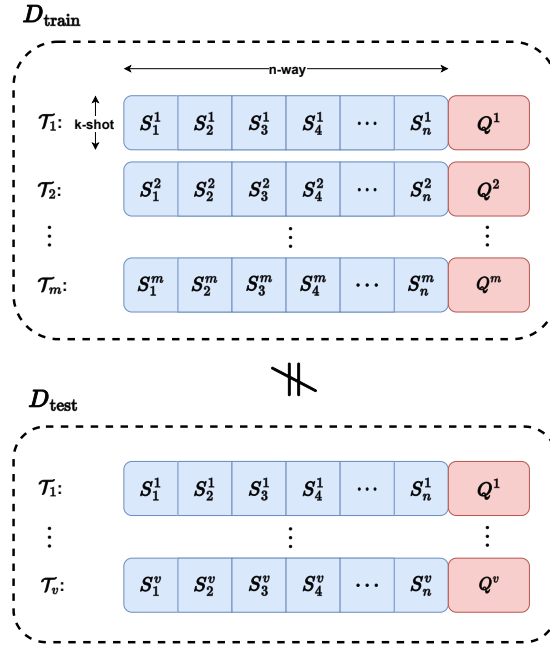


Fig. 1: Formulation of few-shot learning problem including the training set D_{train} with m tasks and the testing set D_{test} with v tasks. Here, m and v could be equal or different. Each task \mathcal{T} comes with different sets of categories and consists of labeled support set S and unlabeled query set Q that share the same categories. Support set S follows the n -way k -shot setting. D_{train} and D_{test} are disjointed in categories. A *few-shot learner* A is trained on D_{train} to perform test on D_{test} .

A few-shot learning problem is usually trained with an episodic learning strategy, where the proposed approach is trained and tested on different tasks with different sets of categories. The episodic learning with m tasks is generally described in Figure 1. Individual task $\mathcal{T} = \{S, Q\} \sim p(D)$ is derived randomly from data set D , where D can be either the training set D_{train} or testing set D_{test} depending on the training scheme and $p(D)$ is the distribution over D . Each task \mathcal{T} consists of two sub-sets: labeled support set S and unlabeled query set Q that share the same n ground-truth categories. Task $\mathcal{T} = \{S, Q\}$ is also

called *episodic batch* or episode for short. One training epoch may contain many different episodes.

Let (x, y) be defined as the input image sample and its ground-truth, respectively. The objective for a few-shot classification task is to predict labels of the query set $Q = \{\mathbf{x}_q^i\}_{i=1}^q$, given the support set $S = \{(\mathbf{x}_s, y_s)^{i,j}\}_{i=1, \dots, n}^{j=1, \dots, k}$, where $y_s \in C$ for a set of n categories (n -way), k is the number of training samples per category (k -shot), and q is the total number of Q samples. The number of k must be small in a few-shot setting. In this paper, we explore two configurations: 5-way 5-shot and 5-way 1-shot. The few-shot classification problem can be formulated with the following optimization function:

$$\theta^* = \arg \min_{\theta} \mathbb{E}_{(S, Q) \sim p(D)} \mathcal{L}(S, Q; A(\cdot | \theta)), \quad (1)$$

$$\mathcal{L}(S, Q; A(\cdot | \theta)) = \frac{1}{q} \sum_{(\mathbf{x}_q, y) \in Q} -\log [p(y | A(\mathbf{x}_q | \theta); S)] + \lambda R(\theta),$$

where $p(y | A(\mathbf{x}_q | \theta); S)$ is the probabilistic prediction of sample $\mathbf{x}_q \in Q$ on true label y using few-shot algorithm $A(\cdot | \theta)$ given for \mathbf{x}_q and support set S . $\lambda R(\theta)$ is an optional regularization with factor λ . The loss function $\mathcal{L}(S, Q; A(\cdot | \theta))$ is dependent on the few-shot problem and method. In this work, the categorical cross-entropy loss is explored for categorical classification.

3.2 Few-Shot Cosine Transformer (FS-CT) Architecture

In this section, we describe the proposed Few-Shot Cosine Transformer (FS-CT) architecture, which utilizes transformer framework to learn the similarities between labeled support and unlabeled query features to recognize query samples following the transductive learning approach. Figure 2 presents the overall architecture of FS-CT, with two main components: learnable prototypical embedding, and Cosine Transformer.

Overall, FS-CT shares a similar architecture with the transformer encoder architecture. Given two input support set S and query set Q , their images are fed into a backbone feature extractor to obtain two feature tensors Z_S and Z_Q , and then features from Z_S are averaged along individual categories to obtain the prototypical representation Z_P like the prototypical network [32]. Unlike other conventional transformer-based architectures, positional encoding is removed, since the arrangement of features is unimportance. After that, Z_P and Z_Q are brought into three linear layers to split into a multi-head of three features $\langle \mathbf{q}^*,$

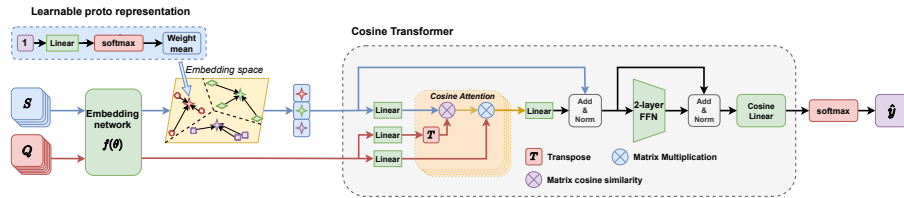


Fig. 2: The overall architecture of the proposed Few-shot Cosine Transformer, which includes two main components: (a) *learnable prototypical embedding* that calculates the categorical proto representation given random support features that might be either in the far margin of the distribution or very close to each other and (b) *Cosine transformer* that determines the similarity matrix between proto representations and query samples for the few-shot classification tasks. The heart of the transformer architecture is *Cosine attention*, an attention mechanism with cosine similarity and no softmax function to deal with two different sets of features. The Cosine transformer shares a similar architecture with a standard transformer encoder block, with two skip connections to preserve information, a two-layer feed-forward network, and layer normalization between them to reduce noise. The outcome value is through a cosine linear layer, with cosine similarity replacing the dot-product, before feeding to softmax for query prediction.

\mathbf{k}, \mathbf{v})⁴, then go through a multi-head cross-attention mechanism to obtain the weight attention features of Z_Q on Z_P . Instead of using the vanilla softmax attention, we propose a variation of the attention mechanism named “*cosine attention*”, which utilizes cosine similarity to calculate the attention weight. The outcome attention values between heads are then fed to an output linear layer to combine heads together, followed by a two-layer MLP with GELU activation function. Two skip-connected layers are applied to prevent losing information and layer normalization is applied before the linear layer for smoothing values throughout the FS-CT. Finally, the outcome feature is brought through a Cosine linear layer followed by the softmax to yield probabilistic scores on individual categories to predict queries’ labels. In the following subsections, we will describe in detail the essential modules within our FS-CT method.

3.3 Learnable Prototypical representation

Given support set $S = (X_S, Y_S)$ and query set $Q = (X_Q, Y_Q)$ follows few-shot setting (n -way, k -shot, q query samples) with $Y_S, Y_Q \in n$ categories; $X_S, X_Q \in \mathbb{R}^{c \times h \times w}$; X_S and X_Q are first fed to a backbone feature extraction $f(\cdot | \theta)$ to

⁴ To avoid the conflict from double usage of the term “query”, we denote the queries \mathbf{q}^* of the attention mechanism to distinguish with the query set Q with sample size q in the few-shot tasks.

obtain the feature representations $Z_S \in \mathbb{R}^{n \times k \times d}$, $Z_Q \in \mathbb{R}^{q \times d}$. Then, all k learned features $\{z_c^i\} \in Z_S$, $i \in [1, k]$ that share the same category c are then average equally (arithmetic mean) to obtain the prototypical representation $Z_P \in \mathbb{R}^{n \times d}$, with $z_c \in Z_P$ represented for the centroid of category c . However, with the few supporting samples chosen randomly, the prototypical representations are not guaranteed to be well represented using this arithmetic mean approach. This may happen when the embeddings of chosen samples are in the far margin of the categorical distribution space or close to each other (see Figure 2). This problem becomes critical when the number of shots is low. To tackle the problem, we developed a learnable averaging method to obtain the prototypical feature for each category that represents better with given data as follows.

$$z_P = \sum_{i=1}^k z_s^i \cdot \text{Softmax}[g(a | \theta_P)]. \quad (2)$$

Initially, the averaging weights $W_{avg} = g(a | \theta_P)$ for calculating categories' centroid are obtained by feeding a fixed scalar input a into the linear layer $g(\cdot | \theta_P)$ with learnable weight $\theta_P \in \mathbb{R}^{n \times k \times 1}$ and no bias. We used $a = 1$ so that the output W_{avg} can have the same value with the weight θ_P . After achieving the averaging weight, Softmax is applied along the k axis to ensure that components within that axis form the weight distribution with the sum of 1. Then, the prototypical representation $Z_P \in \mathbb{R}^{n \times d}$ is obtained by element-wise multiplication between $Z_s \in \mathbb{R}^{n \times k \times d}$ and $W_{avg} \in \mathbb{R}^{n \times k \times 1}$, then summarize values along the k axis to achieve the weight averaging representation on each category, which is the prototypical representation.

In our implementation, instead of feeding a fixed scalar into a linear layer, we directly initiate a learnable parameter with value $a = 1$ that shares the same dimensional space $\mathbb{R}^{n \times k \times d}$ and fed it to a softmax function for W_{avg} . We used the initial value of 1 for the learnable parameter as we want to begin with averaging equally among feature vectors within the same category at first, but then weight values $w \in W_{avg}$ will vary through the training process to obtain a better prototypical representation that fits best with given data. In the experiment, this learnable averaging approach helps us achieve a better representation, and thus comes with higher performances in many scenarios.

3.4 Cosine Transformer

Cosine similarity between two matrices Given two vectors $\mathbf{a}, \mathbf{b} \in \mathbb{R}^n$, the cosine similarity score between \mathbf{a} and \mathbf{b} is calculated by the dot-product of two vectors divided by the product of their magnitudes, as follows.

$$S_C(\mathbf{a}, \mathbf{b}) = \frac{\mathbf{a} \cdot \mathbf{b}}{\|\mathbf{a}\| \cdot \|\mathbf{b}\|} = \frac{\sum_{i=1}^n a_i \cdot b_i}{\sqrt{\sum_{i=1}^n a_i^2} \cdot \sqrt{\sum_{i=1}^n b_i^2}}. \quad (3)$$

From the definition for vectors, we extended the above definition for cosine similarity on matrices. Specifically, the cosine similarity $S_C(A, B) \in \mathbb{R}^{n \times m}$ between matrix $A \in \mathbb{R}^{n \times k}$ and $B \in \mathbb{R}^{k \times m}$ is *the Hadamard division* between the matrix multiplication of A and B^\top and the outer product between vectors $M_A \in \mathbb{R}^n$ and $M_{B^\top} \in \mathbb{R}^m$, where M_A and M_{B^\top} are the vectorization of *the magnitude values of the row vectors* of two matrices A and B^\top , respectively. The definition is described by the formula

$$\begin{aligned} S_C(A, B) &= (A \cdot B) \oslash (M_A \otimes M_{B^\top}) \\ &= (A \cdot B) \oslash \left(\left[\sqrt{\sum_{i=1}^k a_{1,i}^2}, \dots, \sqrt{\sum_{i=1}^k a_{n,i}^2} \right] \right. \\ &\quad \left. \otimes \left[\sqrt{\sum_{i=1}^k b_{i,1}^2}, \dots, \sqrt{\sum_{i=1}^k b_{i,m}^2} \right] \right). \end{aligned} \quad (4)$$

With that definition, individual element $S_C(A, B)_{i,j}$ is *the cosine similarity score* between the row vector a_i of matrix A and the column vector b_j of matrix B , where $i \in [1, n]$, $j \in [1, m]$.

Cosine attention mechanism Initially, as n and q are different in values, we reshaped the proto-feature $Z_P \in \mathbb{R}^{n \times d}$ into the $1 \times n \times d$ tensor and $Z_Q \in \mathbb{R}^{q \times d}$ into a $q \times 1 \times d$ tensor so we can maintain both n and q dimensions in the attention output $h_a \in \mathbb{R}^{q \times n \times d}$, providing the similarity matrix between Z_P and Z_Q . With the two reshaped tensors, a set of three representations $\langle \mathbf{q}^*, \mathbf{k}, \mathbf{v} \rangle$ are obtained by linear layers: $\mathbf{q}^* = Z_P \cdot \theta_{q^*}^\top$; $\mathbf{k} = Z_Q \cdot \theta_k^\top$; $\mathbf{v} = Z_Q \cdot \theta_v^\top$ where $\theta_{q^*}, \theta_k, \theta_v \in \mathbb{R}^{d \times d_h}$ are the weight matrices, d_h is the dimension inside attention. The output attention head h_a can be calculated using the scaled dot-product or “softmax attention” by

$$\text{Softmax attention} = \mathcal{A} \cdot \mathbf{v} = \text{sm} \left[(\mathbf{q}^* \cdot \mathbf{k}^\top) / \sqrt{d} \right] \cdot \mathbf{v} \quad (5)$$

Specifically, in the softmax attention, the matrix multiplication performs dot-product operation between every pair of feature vectors between \mathbf{q}^* and \mathbf{k}^\top , then divided by a scaling factor \sqrt{d} before feeding to a softmax function for an attention map $\mathcal{A} \in \mathbb{R}^{q \times n \times 1}$. The core of the softmax attention is the dot product operation, which calculates the similarity involving vector angle and length (magnitude). The involvement of feature length comes with limitations. First, the feature magnitude is a distinguishing yet unimportant factor in calculating attention, and the similarity output map can become unstable when feature magnitudes vary. This can be critical when \mathbf{q} and \mathbf{k} come from two distributions, few-shot support and query sets respectively. Second, the enlarging in magnitude makes the softmax function produces an extremely small gradient output, thus leading to gradient vanishing [37]. While the division of the fixed scaling

factor \sqrt{d} in softmax attention helps counter this phenomenon, the differential in feature magnitudes still remains.

Therefore, to remove the effect of the differences in vectors’ magnitude, we replaced the dot-product with cosine similarity for calculating \mathcal{A} . We clarify that the concept of replacing the dot-product operation with cosine similarity is not new and has been studied in [24] and applied in few-shot image classification in [5, 13] in terms of a cosine similarity-based classification/recognition model. In this study, the replacement of cosine similarity in the attention mechanism helps us highlight the alignment between two representations by features’ content. Specifically, instead of using a fixed number for scaling the entire weight matrix, individual components of the multiplied matrix will be divided with the product of their corresponding vector’s magnitude. We refer to this attention mechanism as “Cosine Attention” with the general formula described as follows, based on the definition of cosine similarity for matrices in the above section

$$\text{Cosine attention} = [(\mathbf{q}^* \cdot \mathbf{k}^\top) \oslash (M_{\mathbf{q}^*} \otimes M_{\mathbf{k}})] \cdot \mathbf{v} \quad (6)$$

With cosine similarity, the attention map \mathcal{A} focuses more on the features’ content and determines a better attention matrix between every pair of features $\langle q_i^* \in \mathbf{q}^*, k_j \in \mathbf{k}^\top \rangle$. Furthermore, the output distribution of cosine attention can be stable even if its input magnitude varies [24]. By removing the magnitude, the output of cosine similarity is bounded into the range of $[-1, 1]$, indicating the similarity between two features. Thus, Softmax function is no longer necessary for scaling the values. Without the softmax, attention map \mathcal{A} still maintains the probabilistic distributions in the row vectors as well as its components’ ratio. Moreover, as cosine similarity does not scale the weight distributions into the sum of 1, $a_{i,j} \in \mathcal{A}$ possesses a wider range of value. This helps emphasize query features on aligned categories in h_a and vice versa, hence boosting the model’s performances. In our empirical experiment, removing Softmax in Cosine attention helps increase our proposed FS-CT performance significantly, and normalizing \mathbf{q} and \mathbf{k} before feeding to the Softmax attention does not procedure an attention map as adequate as using the Cosine attention alone.

In our FS-CT method, we apply the multi-head mechanism for cosine attention. The initial three linear layers split Z_P and Z_Q into sets of $\langle \mathbf{q}_t^*, \mathbf{k}_t, \mathbf{v}_t \rangle$ where $t \in [1, 8]$. For each set, a corresponding h_a^t is computed, represented for the projection output in different perspectives. Then, the $H_{out} \in \mathbb{R}^{q \times n \times d}$ is obtained with the output weight matrix $\theta_o \in \mathbb{R}^{d_n \times d}$ by

$$H_{out} = \text{concat}(h_a^t) \cdot \theta_o^\top \quad t = 1, \dots, 8. \quad (7)$$

Cosine linear layer for queries prediction After the attention block, two skip connections are performed on $H_{out} = (Z_P + H_{out}) + \text{FFN}(Z_P + H_{out})$ with

layer normalization before each step. The feed-forward network FFN is a simple two linear layers with GELU [15] activation between. With the final outcome feature $H_{out} \in \mathbb{R}^{q \times n \times d}$, a linear layer with weight $\theta_{out} \in \mathbb{R}^{d \times 1}$ is applied follows by softmax for $P_{out} \in \mathbb{R}^{q \times n}$, which represent the probabilistic prediction for every query features on n categories. Instead of using a conventional linear layer, we used a cosine linear layer from [5]. Instead of performing the dot-product between H_{out} and θ_{out} , cosine similarity is replaced between two L2-normalized tensors, using Equation (3). The replacement of cosine similarity instead of the convention dot-product operation helps us achieve a better prediction score for P_{out} . Overall, the probabilistic prediction $p(c | \mathbf{h}_{q,c}; \theta_{out})$ for representation score $\mathbf{h}_{q,c}$ on label c of query sample \mathbf{x}_q over n categories and the predicted label \hat{y} are calculated by

$$p(c | \mathbf{h}_{q,c}, \theta_{out}) = \frac{\exp[S_C(\mathbf{h}_{q,c}, \theta_{out}^\top)]}{\sum_{i=1}^n \exp[S_C(\mathbf{h}_{q,i}, \theta_{out}^\top)]}$$

$$\hat{y} = \arg \max_c p(c | \mathbf{h}_{q,c}, \theta_{out}). \quad (8)$$

3.5 Episodic training Algorithm

We train our proposed FS-CT method with an episodic learning strategy. For each training step, task $\mathcal{T} = \{S, Q\}$ are selected randomly from D_{train} with n categories. For convenience, all learning parameters are referred to as a general parameter θ . With FS-CT, includes backbone feature extraction $f(\cdot | \theta_f)$, is performed, we obtain the probabilistic prediction $p(y | \mathbf{x}_Q, S; \theta)$ of sample $x_Q \in Q$ on label y given S . Finally, Categorical Cross-Entropy loss is applied to update parameters at the end of each training step by Equation (1). Details of the training strategy are presented in Algorithm 1.

4 Experiment Results

4.1 Datasets and experimental setup

To evaluate our method, we adopt three standardized few-shot image classification datasets *mini-ImageNet* [38], CIFAR-FS [2], and CUB-200 [39]. The *mini-ImageNet* dataset is the subset of ImageNet dataset (ILSVRC-2012) [28] that consists of 100 different categories with 600 image samples per each, each image having the size 84×84 pixels. In our implementation, we used the splits by Ravi and Laroché [27] including 64 training categories, 16 validation categories, and 20 testing categories. *CIFAR-FS* including 100 categories containing 600 images for each label with the size of 32×32 pixels. The splits of this dataset are similar to *mini-ImageNet*. The *CUB-200* dataset contains 200 categories of bird species with 11,788 images of 84×84 pixels, which are divided into 100 categories for

Algorithm 1: FS-CT episodic training algorithm over one training epoch with N tasks (episodic batch). Each task \mathcal{T}_i is chosen randomly from the training set D_{train} with a different set of categories to train and update the general parameter θ of our proposed FS-CT, including the embedding backbone $f(\cdot | \theta_f)$.

Input : Training set D_{train} . The number of learning tasks N .
Learnable parameters θ , learning rate θ

Output: Updated parameters θ

```

for  $i$  in  $\{1, \dots, N\}$  do
1  Randomly chosen task  $\mathcal{T}_i = \{S, Q\} \sim p(D_{\text{train}})$ .
2  Obtain feature representations  $Z_S, Z_Q$  from  $S$  and  $Q$  by the backbone
    $f(\cdot | \theta_f)$ 
3  Calculate the prototypical representation  $Z_P$  using Equation (2).
4  Obtain  $\langle \mathbf{q}^*, \mathbf{k}, \mathbf{v} \rangle$  for attention by:
    $\mathbf{q}^* \leftarrow Z_P \cdot \theta_{q^*}^\top; \mathbf{k} \leftarrow Z_Q \cdot \theta_k^\top; \mathbf{v} \leftarrow Z_Q \cdot \theta_v^\top$ 
5  Calculate  $H_{out}$  by Cosine Attention by Equations (6) and (7).
6  Perform two skip-connections and FFN for Cosine Transformer:
    $H_{out} \leftarrow (Z_P + H_{out}) + \text{linear}(\text{GELU}[\text{linear}(Z_P + H_{out})])$ 
7  Obtain the query prediction scores  $\hat{y}$  with Equation (8).
8  Compute the loss function  $\mathcal{L}$  as in Equation (1).
9  Perform gradient descent step to update the parameter:
    $\theta \leftarrow \theta - \alpha \nabla_\theta \mathcal{L}$ 
end

```

training, 50 categories for validating, and 50 categories for testing.

Besides the three few-shot datasets above, we also created a custom dataset for yoga poses scoring, including 50 categories of main yoga poses with 2,480 images. We developed this small-scale dataset as an initial step for making a smart monitoring and studying scheme for yoga participants. The dataset is partially derived from Kaggle [29] and storage in our implementation code on GitHub⁵. The number of images are ranging from 30 to 81 samples per category with arbitrary size. Furthermore, some categories’ samples are different in view-point, appearance, or visual condition, which makes the dataset become more challenge. We split the dataset into 25 categories for training, 13 categories for validating, and 12 categories for testing. Some example poses of the dataset are presented in Figure 3, with the statistics of the dataset distribution presented in Table 1.

4.2 Implementation Details

We implemented our method and conducted experiments on PyTorch, using a CPU Intel Core i9-10900X 3.7GHz with a GPU NVIDIA GeForce RTX 3090

⁵ <https://github.com/vinuni-vishc/Few-shot-transformer/tree/main/dataset/Yoga>



Fig. 3: Several exemplary samples for categorial poses of the yoga poses dataset, consisting of 50 different poses with a total of 2,480 images.

Table 1: Statistical description of the custom image dataset for Yoga poses over three main sets for training, validation, and testing few-shot image classification method.

	Train	Val	Test	Total
Number of Categories	25	13	12	50
Min number of samples per category	30	39	31	30
Max number of samples per category	80	81	67	81
Average of samples per category	50.2	49.9	48.0	49.6
Total samples	1,255	649	576	2,480

24GB and 16GB RAM memory. Methods were trained and experimented with the learning rate 0.001, weight decay 1×10^{-5} , and AdamW [22] optimization function, and no dropout. We performed two configurations: 5-way 5-shot and 5-way 1-shot, with 16 query samples for each category, making a total of 80 queries. All training steps are trained on 50 training epochs with 200 episodic batches (episodes) for each. Each training epoch is followed by a validating step with 200 episodes to select the best-performed model for the testing phase on 600 episodes. All training, validating, and testing sets are disjointed in categories. To increase training data samples for training models, we applied augmentation, including random resizing, cropping, horizontal flipping, color jittering, and image normalizing. All experiments were conducted in the same common ground of code, setting, and environment for a fair evaluation and comparison.

For backbone feature extraction, we mainly utilized four backbone models Conv4, Conv6, ResNet-18, and ResNet-32 for the experiments. Conv4 and Conv6 are lightweight CNN models with 4 and 6 layers respectively and have been used before in [5, 34, 38] that are trained from scratch. On the other hand, the ResNet backbone networks and pretrained on *mini-ImageNet* are available on Torchvision. However, as the *mini-ImageNet* is a subset of the ImageNet, we deployed a special pre-trained model named FETI [1] for evaluating the dataset, which will be described in detail later. For each type of backbone architecture, we resized sample images before training depending on the dataset and backbone model. Particularly, with CNN backbones, we resize images into 64×64 pixels for CIFAR-FS (due to its small size originally) and 84 pixels for other datasets, and with Res-Net backbones, the resized input image is 112×112 and 224×224 , respectively. For all experiments, we report results in accuracy and use this performance metric for comparisons.

4.3 Ablation study

Evaluation on *mini-ImageNet*, CIFAR-FS and CUB-200 datasets For the experiment, besides FS-CT model, we also deploy another attention-based few-shot learning algorithm CTX [8] as a baseline for the comparison with our proposed FS-CT method. We utilized both Softmax attention and Cosine attention for two few-shot methods for our ablation evaluation. The two main experiment results on *mini-ImageNet*, CIFAR-FS, and CUB-200 dataset are presented in Table 2 for the FS-CT method only with two embedding backbones Conv4 and Conv6, and Table 3 for both CTX and FS-CT methods with ResNet-18, and ResNet-32 backbones. Both experiments are conducted in 5-way 1-shot and 5-way 5-shot settings. We use the full ImageNet pre-trained models on ResNet backbones for Table 3 and we will have a separate experiment for a fair evaluation on *mini-ImageNet* in the latter section. Data augmentation is applied for our proposed FS-CT method only.

In general, our FS-CT outperformed CTX in different ResNet backbones, datasets, and few-shot settings. The results are augmented further with the cosine attention mechanism, with the improved performance from nearly 5% to over 20% in various scenarios. Overall, *5-shot learning comes with better performance than 1-shot learning*. This happens typically on few-shot algorithms as more label samples come with better centroid representation for individual categories, thus classifying queries better. Furthermore, *augmentation helps improve classifier performances* on FS-CT, mainly with 5-shot setting. There are some occasions when augmentation does not help improve performance in one-shot learning. This could be explained by augmentation that comes with the growth in noise in categorical representation, therefore affecting the performances on one-shot learning. Augmentation seems to be effective on ResNet backbones, as

Table 2: Performance of our proposed *FS-CT* for 5-way setting on *mini*-ImageNet, CUB-200, and CIFAR-FS, using either the baseline **softmax attention or the proposed **cosine attention** with two shallow backbones **Conv4** and **Conv6** with 50 training epoch and **data augmentation**. Similar to [5], we report the mean of 600 randomly generated test episodic tasks. The best and second best results are **bolded** and underlined, respectively. The evaluation metric is accuracy in percentage.**

Methods	<i>mini</i> -ImageNet				CUB-200				CIFAR-FS			
	Conv4		Conv6		Conv4		Conv6		Conv4		Conv6	
	1-shot	5-shot	1-shot	5-shot	1-shot	5-shot	1-shot	5-shot	1-shot	5-shot	1-shot	5-shot
<i>FS-CT</i> + Softmax Attn (baseline)	<u>42.55</u>	58.08	39.11	56.52	53.44	66.14	<u>55.41</u>	65.87	<u>48.57</u>	66.22	<u>46.66</u>	65.43
<i>FS-CT</i> + Softmax Attn + Aug	38.11	57.14	33.89	54.26	51.50	<u>69.73</u>	48.61	<u>71.62</u>	40.95	64.31	43.74	60.41
<i>FS-CT</i> + Cosine Attn (our)	45.69	60.38	40.52	59.85	56.41	67.12	55.27	66.90	53.86	69.03	51.04	68.76
<i>FS-CT</i> + Cosine Attn + Aug	40.73	<u>60.21</u>	<u>35.33</u>	<u>57.81</u>	<u>56.34</u>	75.88	55.68	76.93	47.85	<u>68.35</u>	45.06	<u>67.40</u>

Table 3: Performance of the baseline *CTX* [8] and our proposed *FS-CT* for 5-way setting on three datasets *mini*-ImageNet, CUB-200, and CIFAR-FS, using either the standard **softmax attention or our proposed **cosine attention**, with two embedding backbones **ResNet-18** and **ResNet-34**, pre-trained on ImageNet. **Data augmentation** is applied for our *FS-CT* method only. Similar to Table 2, we validate the methods with 600 random task episode tasks and report the mean value. The best and second best results are **bolded** and underlined, respectively. The evaluation metric is accuracy in percentage.**

Methods	<i>mini</i> -ImageNet*				CUB-200				CIFAR-FS			
	ResNet-18		ResNet-34		ResNet-18		ResNet-34		ResNet-18		ResNet-34	
	1-shot	5-shot	1-shot	5-shot	1-shot	5-shot	1-shot	5-shot	1-shot	5-shot	1-shot	5-shot
<i>CTX</i> (baseline) + Softmax Attn	62.37	63.09	65.08	65.66	61.24	62.12	64.28	66.02	41.16	43.05	44.54	48.01
<i>CTX</i> + Cosine Attn	<u>77.21</u>	92.18	82.09	<u>93.41</u>	73.14	85.71	76.54	88.15	60.18	73.97	61.82	74.83
<i>FS-CT</i> (our) + Softmax Attn	72.36	84.13	73.90	85.58	74.69	85.38	75.97	87.03	63.40	77.98	63.05	78.04
<i>FS-CT</i> + Cosine Attn	75.93	90.12	79.01	91.64	<u>77.72</u>	<u>89.13</u>	<u>77.72</u>	<u>89.63</u>	<u>64.29</u>	<u>80.57</u>	<u>65.67</u>	<u>81.44</u>
<i>FS-CT</i> + Softmax Attn + Aug	73.84	84.65	74.61	88.74	75.89	88.06	77.01	89.05	62.41	78.17	62.14	79.17
<i>FS-CT</i> + Cosine Attn + Aug	77.40	<u>91.33</u>	<u>80.32</u>	93.82	81.12	91.96	81.23	92.35	64.49	81.46	67.06	82.89

* For *mini*-ImageNet, we will have a different experiment using more suitable pre-trained backbones for a fair comparison.

FS-CT using cosine attention with augmentation mainly achieves the best result within individual scenarios. Across scenarios, *deeper backbones comes with better performances*, as increasing the number of layers helps both CNN and ResNet backbones achieve higher results. Moreover, the models' performance is heavily affected by the choice of backbone, as in most cases, ResNet-34 feature extractor comes with the highest performance among the four. These observations are further illustrated in Figure 4, where the line graphs present the test accuracy

correlations between CTX and FS-CT variants on ResNet-34 backbone across few-shot settings and datasets in Table 3.

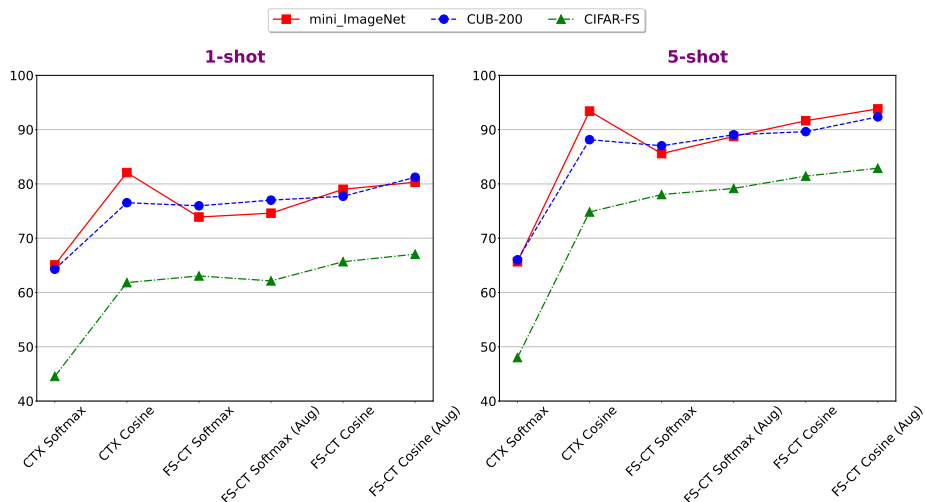


Fig. 4: Testing accuracies between CTX and FS-CT across the three few-shot datasets with Softmax and Cosine attention mechanisms and augmentation for FS-CT, using ResNet-34 as the backbone. Generally, FS-CT achieved higher accuracies than CTX, with the only exception in *mini-ImageNet*, where the performances of CTX are nearly equal (in 5-shot learning) or higher (in 1-shot learning) than FS-CT. However, CTX only achieves these performances with our cosine attention mechanism as the core. Cosine attention improves the performances of two few-shot methods, and data augmentation further enhances them.

Performances of two attention mechanisms Across Table 2 and 3, we can observe that *using cosine attention helps achieve more robust performance than Softmax attention*. This observation is further illustrated in Figure 5, where cosine attention helps both methods acquire a higher accuracy at the starting point, and learn better training graphs across 50 epochs. The two methods’ performances improve significantly as cosine attention produces a more stable attention outcome. Using cosine attention helps improve the learning ability consistently across datasets, settings, and methods compared with the baseline Softmax attention. Additionally, applying Cosine attention without normalizing features is more effective than our early attempts to normalize two input feature sets before Softmax attention by BatchNorm and LayerNorm. This further highlights the robust improvement of our cosine attention for the cross-attention

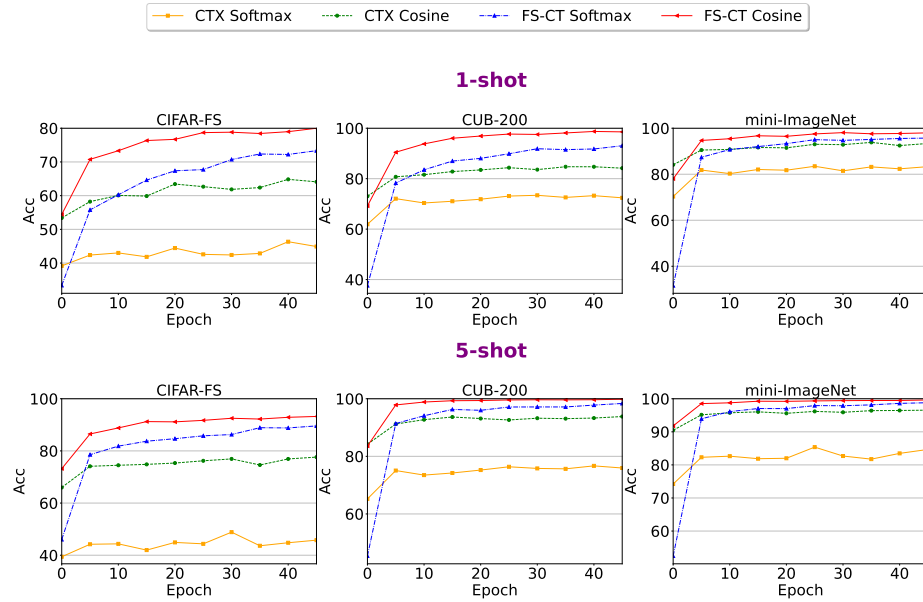


Fig. 5: Training graphs of FS-CT and CTX for 1-shot and 5-shot learning with ResNet-34 backbone, using either the standard *softmax* attention or the proposed *cosine* attention mechanism. Cosine attention significantly improves both few-shot methods among settings and datasets with higher starting points and better training plots. FS-CT achieves better training performances than its counterpart CTX with both attention mechanisms.

mechanism compared with the baseline scaled dot-product attention. Furthermore, the training graphs in Figure 4 and Figure 5 also show that, under the same configuration (dataset, few-shot setting, backbone, and attention mechanism), our FS-CT learns and performs better than the baseline CTX significantly.

Figure 6 illustrates the attention heatmaps between the baseline Softmax attention (top) and the improved Cosine attention (bottom) for 5-way 5-shot learning, from the early training phase (left) to the later training phase (right). Each heatmap point represents the similarity frequency between query samples (x-axis) from one category and the corresponding prototypical representation (y-axis) of the same category. All heatmaps are obtained on the performances from the same few-shot task derived from the testing test of *mini-ImageNet*. Cosine attention results in a more robust heatmap as it generates a stronger similarity matrix between the query and support samples (through proto-representations) that share the same ground truth, standing by the main diagonal. In the early epoch, the attention heatmap procedure by Cosine attention achieves a similar, if not better, than the Softmax attention heatmap from the latter epoch. The

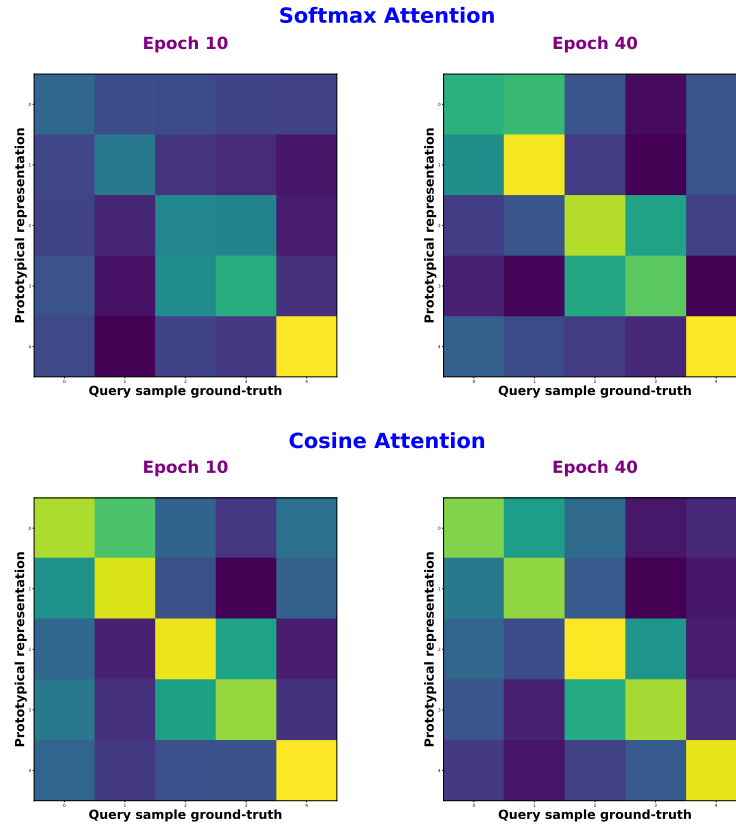


Fig. 6: Attention similarity heatmaps of Softmax attention (top row) and Cosine attention (bottom row) on FS-CT, taken from epoch 10 (left column) and epoch 40 (right column) of the 50-epoch-training process. The attention heatmap is between the query samples and support prototypical representations that share the same ground-truth categories. We use ResNet-34 as backbone embedding with 5-way 5-shot setting and perform on the same few-shot task of the *mini*-ImageNet test set for the heatmap. Cosine attention produces more stable and robust attention heatmaps (through the main diagonal) from the early phase of training and becomes more apparent as the training progresses.

strong connection diagonal between queries and support representations with the same categorical ground-truth becomes more apparent with Cosine attention as training progresses, resulting in a more stable heatmap. This emphasizes the robustness of our improved Cosine attention for the few-shot classification task.

Table 4: Performance of FS-CT on *mini*-ImageNet with a pre-trained model FETI (Feature Extractor Trained (partially) on ImageNet) that was trained with non-test-set overlapping ImageNet classes to avoid the natural advantage of ImageNet pre-trained model. We use two supported backbones ResNet-12 and ResNet-18 for the pre-trained model, with the same validating scheme and configurations.

Methods	<i>mini</i> -ImageNet			
	ResNet-12		ResNet-18	
	1-shot	5-shot	1-shot	5-shot
<i>FS-CT</i> (FETI) + Softmax Attn	45.70	57.03	40.06	58.20
<i>FS-CT</i> (FETI) + Cosine Attn	55.62	70.36	41.84	71.34
<i>FS-CT</i> (FETI) + Softmax Attn + Aug	38.88	57.16	47.72	62.71
<i>FS-CT</i> (FETI) + Cosine Attn + Aug	49.39	73.00	55.67	73.42

Performances of FS-CT on *mini*-ImageNet with partially pre-trained model As *mini*-ImageNet dataset is a subset of the ImageNet dataset, using a default pre-trained ResNet on the full ImageNet as feature extraction comes with a natural advanced performance on the few-shot *mini*-ImageNet dataset, as shown with very high performance in Table 3. Therefore, it is unfair for us if we want to compare our FS-CT performances with other few-shot classification methods. To tackle the problem, we used a specific pre-trained model that had been trained on a separated ImageNet subset with the *mini*-ImageNet testing set. We adapted this pre-trained model, called “Feature Extractor Trained (partially) on ImageNet” or FETI in abbreviation, from [1]. Because the pre-trained model was trained only on ResNet-18, we used two backbone models ResNet-18 and ResNet-12, as ResNet-32 is too different in layer number and layer size, and ResNet-12 is roughly adequate with ResNet-18 in architecture. Table 4 shows our FS-CT performance on *mini*-ImageNet with FETI pre-trained model. In general, the performances are reduced in the comparison with results from Table 3. This emphasizes the necessity of having a good embedding through a pre-trained model, in order to address the few-shot problem, as pointed out in [7, 36]. Results show that FS-CT with Cosine attention still outperformed the baseline Softmax attention, demonstrating the robust learning capability of our proposed attention mechanism.

Evaluation on Yoga poses dataset For the custom Yoga poses dataset, the results are separately presented in Table 5. While Cosine attention still comes with more robust performances than the baseline Softmax attention, augmentation overall seems not to help the method in improving the outcome results.

Table 5: Evaluation of the baseline CTX and our proposed FS-CT on the custom Yoga dataset using two backbones ResNet-18 and ResNet-34 with 50 training epochs and 600 random testing tasks. The best and second best results are **bolded** and underlined, respectively. The evaluation metric is accuracy in percentage.

Methods	Yoga Dataset			
	ResNet-18		ResNet-34	
	1-shot	5-shot	1-shot	5-shot
<i>CTX</i> (baseline) + Softmax Attn	49.83	54.88	53.09	55.44
<i>CTX</i> + Cosine Attn	59.99	<u>76.61</u>	<u>63.12</u>	<u>77.80</u>
<i>FS-CT</i> (our) + Softmax Attn	<u>61.40</u>	69.15	58.89	71.12
<i>FS-CT</i> + Softmax Attn + Aug	51.89	66.21	55.08	70.12
<i>FS-CT</i> + Cosine Attn.	66.38	80.34	64.32	77.66
<i>FS-CT</i> + Cosine Attn + Aug	57.98	73.58	59.76	77.92

Our theory is that this phenomenon is affected by the significant difference in variations within the same pose category. We are aiming to invest deeper into the dataset on further studies for prospective applications in Yoga monitoring research for healthcare.

5 Discussion

We have proposed a transformer-based method for a few-shot classification task with an attention mechanism using cosine similarity. While our results in various few-shot datasets are promising, there are some limitations. First, our method’s performances highly depend on the choice of embedding backbone, particularly those with a pre-trained model. Second, the complexity of architecture may prevent FS-CT from reaching higher performance levels. Although skip-connection was used to preserve information, it is possible that this was insufficient. Many few-shot approaches, including those from [5, 32, 34, 38] share a straightforward pipeline but perform well across few-shot datasets. We want to continue this line of research. Third, while we consider our improved learnable prototypical embedding is a simple method to address the support variation challenge in few-shot learning, further investigation should be done to shed the light on our improvement. Moreover, we believe that more efficient improvements to the prototype network are yet to be discovered. Last, we are only able to directly compare our proposed cosine attention to the scaled dot-product attention because of the limitation in resources. Recent research has proposed a variety of attention mechanisms, and future studies should be conducted on a wider variety of attention

mechanisms on various few-shot problems (not just limited to the classification task). We leave these limitations for our future studies.

6 Conclusion

We introduced in this research FS-CT, a novel transductive learning method for the few-shot image classification task using prototype network and transformer architecture. Initially, our method retrieves the centroid feature of individual categories from the support set for prototypical representations. To improve the quality of the centroids' representation, we made this process learnable with adjustable weights. The two prototypical representations and query features are then fed into a transformer-based framework with cross-attention mechanism for few-shot classification. Rather than designing a new architecture for the transformer, we focus on improving the attention layer for better learning ability. This leads to the development of a novel attention mechanism called Cosine attention, aiming to remove the magnitude disparities from two sets of input features, resulting in a more steady, robust attention outcome. Through experiments, we surpassed the baseline scaled dot-product attention with our proposed Cosine attention in various configurations, and our few-shot classification approach FS-CT achieved comparable performances on many few-shot datasets.

References

1. Bateni, P., Barber, J., van de Meent, J.W., Wood, F.: Enhancing few-shot image classification with unlabelled examples. In: Proceedings of the IEEE/CVF Winter Conference on Applications of Computer Vision. pp. 2796–2805 (2022)
2. Bertinetto, L., Henriques, J.F., Torr, P.H., Vedaldi, A.: Meta-learning with differentiable closed-form solvers. arXiv preprint arXiv:1805.08136 (2018)
3. Boudiaf, M., Ziko, I., Rony, J., Dolz, J., Piantanida, P., Ben Ayed, I.: Information maximization for few-shot learning. *Advances in Neural Information Processing Systems* **33**, 2445–2457 (2020)
4. Carion, N., Massa, F., Synnaeve, G., Usunier, N., Kirillov, A., Zagoruyko, S.: End-to-end object detection with transformers. In: European conference on computer vision. pp. 213–229. Springer (2020)
5. Chen, W.Y., Liu, Y.C., Kira, Z., Wang, Y.C., Huang, J.B.: A closer look at few-shot classification. In: International Conference on Learning Representations (2019)
6. Cheng, B., Schwing, A., Kirillov, A.: Per-pixel classification is not all you need for semantic segmentation. *Advances in Neural Information Processing Systems* **34**, 17864–17875 (2021)
7. Chowdhury, A., Jiang, M., Chaudhuri, S., Jermaine, C.: Few-shot image classification: Just use a library of pre-trained feature extractors and a simple classifier. In: Proceedings of the IEEE/CVF International Conference on Computer Vision. pp. 9445–9454 (2021)

8. Doersch, C., Gupta, A., Zisserman, A.: Crosstransformers: spatially-aware few-shot transfer. *Advances in Neural Information Processing Systems* **33**, 21981–21993 (2020)
9. Dosovitskiy, A., Beyer, L., Kolesnikov, A., Weissenborn, D., Zhai, X., Unterthiner, T., Dehghani, M., Minderer, M., Heigold, G., Gelly, S., et al.: An image is worth 16x16 words: Transformers for image recognition at scale. *arXiv preprint arXiv:2010.11929* (2020)
10. Fei-Fei, L., Fergus, R., Perona, P.: One-shot learning of object categories. *IEEE transactions on pattern analysis and machine intelligence* **28**(4), 594–611 (2006)
11. Finn, C., Abbeel, P., Levine, S.: Model-agnostic meta-learning for fast adaptation of deep networks. In: *International conference on machine learning*. pp. 1126–1135. PMLR (2017)
12. Finn, C., Xu, K., Levine, S.: Probabilistic model-agnostic meta-learning. *Advances in neural information processing systems* **31** (2018)
13. Gidaris, S., Komodakis, N.: Dynamic few-shot visual learning without forgetting. In: *Proceedings of the IEEE conference on computer vision and pattern recognition*. pp. 4367–4375 (2018)
14. Han, G., Ma, J., Huang, S., Chen, L., Chang, S.F.: Few-shot object detection with fully cross-transformer. In: *Proceedings of the IEEE/CVF Conference on Computer Vision and Pattern Recognition*. pp. 5321–5330 (2022)
15. Hendrycks, D., Gimpel, K.: Gaussian error linear units (gelus). *arXiv preprint arXiv:1606.08415* (2016)
16. Hou, R., Chang, H., Ma, B., Shan, S., Chen, X.: Cross attention network for few-shot classification. *Advances in Neural Information Processing Systems* **32** (2019)
17. Kotia, J., Kotwal, A., Bharti, R., Mangrulkar, R.: Few shot learning for medical imaging. In: *Machine learning algorithms for industrial applications*, pp. 107–132. Springer (2021)
18. Lake, B.M., Salakhutdinov, R., Tenenbaum, J.B.: Human-level concept learning through probabilistic program induction. *Science* **350**(6266), 1332–1338 (2015)
19. Lee, Y., Choi, S.: Gradient-based meta-learning with learned layerwise metric and subspace. In: *International Conference on Machine Learning*. pp. 2927–2936. PMLR (2018)
20. Liu, L., Hamilton, W., Long, G., Jiang, J., Larochelle, H.: A universal representation transformer layer for few-shot image classification. *9th International Conference on Learning Representations, ICLR* (2021)
21. Liu, Y., Lee, J., Park, M., Kim, S., Yang, E., Hwang, S.J., Yang, Y.: Learning to propagate labels: Transductive propagation network for few-shot learning. *arXiv preprint arXiv:1805.10002* (2018)
22. Loshchilov, I., Hutter, F.: Decoupled weight decay regularization. *arXiv preprint arXiv:1711.05101* (2017)
23. Lu, Y., Yu, F., Reddy, M.K.K., Wang, Y.: Few-shot scene-adaptive anomaly detection. In: *European Conference on Computer Vision*. pp. 125–141. Springer (2020)
24. Luo, C., Zhan, J., Xue, X., Wang, L., Ren, R., Yang, Q.: Cosine normalization: Using cosine similarity instead of dot product in neural networks. In: *International Conference on Artificial Neural Networks*. pp. 382–391. Springer (2018)

25. Qiao, L., Shi, Y., Li, J., Wang, Y., Huang, T., Tian, Y.: Transductive episodic-wise adaptive metric for few-shot learning. In: Proceedings of the IEEE/CVF international conference on computer vision. pp. 3603–3612 (2019)
26. Qiao, S., Liu, C., Shen, W., Yuille, A.L.: Few-shot image recognition by predicting parameters from activations. In: Proceedings of the IEEE Conference on Computer Vision and Pattern Recognition. pp. 7229–7238 (2018)
27. Ravi, S., Larochelle, H.: Optimization as a model for few-shot learning. In: In International Conference on Learning Representations (ICLR) (2017)
28. Russakovsky, O., Deng, J., Su, H., Krause, J., Satheesh, S., Ma, S., Huang, Z., Karpathy, A., Khosla, A., Bernstein, M., et al.: Imagenet large scale visual recognition challenge. *International journal of computer vision* **115**(3), 211–252 (2015)
29. Saxena, S.: Yoga pose image classification dataset (2020), [Last accessed on 2 August 2022]. Available online: <https://www.kaggle.com/shrutisaxena/yoga-pose-image-classification-dataset>
30. Shao, S., Xing, L., Wang, Y., Xu, R., Zhao, C., Wang, Y., Liu, B.: Mhfc: Multi-head feature collaboration for few-shot learning. In: Proceedings of the 29th ACM international conference on multimedia. pp. 4193–4201 (2021)
31. Sheynin, S., Benaim, S., Wolf, L.: A hierarchical transformation-discriminating generative model for few shot anomaly detection. In: Proceedings of the IEEE/CVF International Conference on Computer Vision. pp. 8495–8504 (2021)
32. Snell, J., Swersky, K., Zemel, R.: Prototypical networks for few-shot learning. *Advances in neural information processing systems* **30** (2017)
33. Sun, Q., Liu, Y., Chua, T.S., Schiele, B.: Meta-transfer learning for few-shot learning. In: Proceedings of the IEEE/CVF Conference on Computer Vision and Pattern Recognition. pp. 403–412 (2019)
34. Sung, F., Yang, Y., Zhang, L., Xiang, T., Torr, P.H., Hospedales, T.M.: Learning to compare: Relation network for few-shot learning. In: Proceedings of the IEEE conference on computer vision and pattern recognition. pp. 1199–1208 (2018)
35. Tang, H., Liu, X., Sun, S., Yan, X., Xie, X.: Recurrent mask refinement for few-shot medical image segmentation. In: Proceedings of the IEEE/CVF International Conference on Computer Vision. pp. 3918–3928 (2021)
36. Tian, Y., Wang, Y., Krishnan, D., Tenenbaum, J.B., Isola, P.: Rethinking few-shot image classification: a good embedding is all you need? In: European Conference on Computer Vision. pp. 266–282. Springer (2020)
37. Vaswani, A., Shazeer, N., Parmar, N., Uszkoreit, J., Jones, L., Gomez, A.N., Kaiser, L., Polosukhin, I.: Attention is all you need. *Advances in neural information processing systems* **30** (2017)
38. Vinyals, O., Blundell, C., Lillicrap, T., Wierstra, D., et al.: Matching networks for one shot learning. *Advances in neural information processing systems* **29** (2016)
39. Wah, C., Branson, S., Welinder, P., Perona, P., Belongie, S.: The caltech-ucsd birds-200-2011 dataset. California Institute of Technology (2011)
40. Wang, Y.X., Girshick, R., Hebert, M., Hariharan, B.: Low-shot learning from imaginary data. In: Proceedings of the IEEE conference on computer vision and pattern recognition. pp. 7278–7286 (2018)

41. Ye, H.J., Hu, H., Zhan, D.C., Sha, F.: Few-shot learning via embedding adaptation with set-to-set functions. In: Proceedings of the IEEE/CVF Conference on Computer Vision and Pattern Recognition. pp. 8808–8817 (2020)
42. Yu, Y., Bian, N.: An intrusion detection method using few-shot learning. *IEEE Access* **8**, 49730–49740 (2020)
43. Yuan, S., Zheng, P., Wu, X., Tong, H.: Few-shot insider threat detection. In: Proceedings of the 29th ACM International Conference on Information & Knowledge Management. pp. 2289–2292 (2020)
44. Zhang, G., Kang, G., Yang, Y., Wei, Y.: Few-shot segmentation via cycle-consistent transformer. *Advances in Neural Information Processing Systems* **34**, 21984–21996 (2021)
45. Zhang, X., Meng, D., Gouk, H., Hospedales, T.M.: Shallow bayesian meta learning for real-world few-shot recognition. In: Proceedings of the IEEE/CVF International Conference on Computer Vision. pp. 651–660 (2021)